Ab initio study of the nonlinear optical susceptibility of TeO_2-based glasses

A. P. Mirgorodsky,* M. Soulis, P. Thomas, and T. Merle-Méjean
Laboratoire de Science des Procédés Céramiques et de Traitements de Surface UMR 6638 CNRS, Faculté des Sciences, Université de Limoges, 123, avenue Albert Thomas, 87060 Limoges Cedex, France

M. Smirnov
Fock Institute of Physics, Saint-Petersburg University, 194508 Petrodvoretz, Saint-Petersburg, Russia
(Received 5 September 2005; revised manuscript received 22 December 2005; published 28 April 2006)

To gain a better insight into the origin of the outstanding nonlinear optic susceptibilities of TeO_2-based glasses whose numerical characteristics are almost two orders of magnitude higher than those of SiO_2-based glasses, a comparative computer simulation of their dielectric properties was performed using *ab initio* studies of a series of $(SiO_2)_p$ and $(TeO_2)_p$ polymer molecules. This comparison showed that these properties are reproducible only in a TeO_2 glass simulated as an ensemble of chainlike $(TeO_2)_p$ polymer molecules with $p \rightarrow \infty$, which was interpreted as evidence for the essential nonlocality of the electronic polarizability mechanism in that glass. The relevant model calculations showed the reasonableness of this hypothesis, which was subsequently used to explain the influence of modifier content on the nonlinear optic susceptibility of the tellurite glasses.

DOI: 10.1103/PhysRevB.73.134206 PACS number(s): 61.43.Fs, 61.43.Bn

I. INTRODUCTION

In 1988 Hall *et al.* discovered[1] that oxide glasses can have very high nonlinear optical (NLO) characteristics comparable to those of chalcogenide glasses which were considered at that time as the most nonlinear optic materials. Since then, a large amount of research has been devoted to NLO properties of oxide glasses of various compositions. Therefore, it was found that those properties are best exhibited by TeO_2-based glasses which offer exceptionally high nonlinear susceptibilities.[2–11] In particular, one of the greatest hypersusceptibilities of oxide glasses presently known is that of pure TeO_2 glass (50 times higher than that of pure SiO_2 glass[8]). Although, as a rule, this characteristic becomes less pronounced in tellurite glasses, and its value markedly decreases with increasing modifier concentration, tellurite glasses are regarded as rather (if not the best) promising materials for NLO devices.

Attempts to understand the origin of the remarkable NLO properties of TeO_2-based glasses have been undertook in a series of theoretical studies. Some of them[3,8,9] were based on semiempirical theoretical models;[12–14] others used quantum-mechanical calculations for small finite clusters having TeO_4 and TeO_3 fragments.[3,6,10,15] None of them seem to be methodologically and physically self-consistent. Actually, the former studies took Lines' approach[12–14] concentrating on the role of *d* electrons and ignoring the presence of electron lone pairs, which can hardly be adequate for electronic properties of structures involving atoms of tellurium and oxygen. The latter studies suppose that the hyperpolarizability mechanism of telluria-based glasses is localized within the first Te—O coordination sphere, thus ignoring the experimental evidence unequivocally indicating an intimate linkage among that mechanism and glass polymerization; in other words, the effects of electron delocalization are not active here.

It can be added that in no case were the results of the above mentioned theoretical studies compared quantitatively with the actual properties of TeO_2-based glasses. So whether these studies were capable of reproducing the given experimental data, thus providing some progress toward the understanding of its origin, is still an open question. Consequently, an insight into the nature of the NLO properties of the TeO_2-based glasses remains a challenge for fundamental solid state physics and chemistry.

Although the quantum-mechanics calculation techniques seem to be the most adequate tool for attacking this problem, it should be clearly understood that in principle such calculations are basically capable of providing numerical characterization of the electronic properties of matter rather than directly revealing their "driving forces." It can be recalled that the physical transparency which is so attractive in many empirical models as a rule is lost in *ab initio* quantum-mechanical calculations which, in fact, represent a kind of "computer experiment." Thus, from the methodological point of view, the program of any *ab initio* study aiming to explain particular properties of a given material should be based on some initial hypothesis and ideas which can be confirmed (or rejected) by computer simulation in considering a standard "structure-property" problem.

The recent *ab initio* calculations of the structural and vibrational properties of the $(TeO_2)_p$ polymers[16] complemented by lattice-dynamical studies of different crystalline polymorphs of TeO_2 (Ref. 17) made it possible to think that chainlike clusters framed from the Te—O—Te bridges and Te—O terminal bonds are the most adequate models of the structural fragments of pure TeO_2 glass.

The central hypothesis of the present study was that the high nonlinear optic susceptibility of TeO_2 glass comes from electron delocalization effects within these chains. We wanted to answer the following questions.

(1) Is this the case?

(2) Does the NLO susceptibilty of TeO_2 glass depend on the size of the structural fragments forming the glass framework?

(3) Why are the NLO characteristics of SiO_2 glass (in which a polymerization through Si—O—Si bridges occurs) much weaker than those of TeO_2 glass?

(4) In what way does the modifier concentration influence the NLO susceptibility mechanism in tellurite glasses?

In order to reach this objective, a comprehensive *ab initio* calculation of various $(SiO_2)_p$ and $(TeO_2)_p$ polymer clusters was performed with the emphasis on their linear and nonlinear polarizabilities which were used to simulate the linear and NLO susceptibilities of SiO_2 and TeO_2 glasses by employing the model technique described below in Sec. III. Additionally, a series of experimental data on the NLO susceptibility of alkaline tellurite glasses were treated in a similar way. So, to our knowledge, the present work is the first joint theoretical study of the NLO properties of SiO_2 and TeO_2-based glasses, based on the comparison of the measured values and the *ab initio* simulation.

The paper is organized as follows. Section II is mainly devoted to experimental data on the NLO properties of the glasses in question, and concerns a particular problem customarily arising in this domain: namely, how the properties measured for different light frequencies can be interrelated and compared to those calculated for static electric fields. Section III provides details about the theoretical scheme used in this paper; Sec. IV summarizes the results of the calculations. They are discussed in Sec. V, giving rise to some further hypotheses and ideas. Final conclusions are in Sec. VI.

II. OPTICAL SUSCEPTIBILITIES OF TeO_2- AND SiO_2-BASED GLASSES

The polarization produced by a macroscopic electric field **E** occurring in a homogeneous material is specified by the polarization vector **P** (dipole moment per unit volume) whose Cartesian components P_i are generally described as functions of the field components E_i $(i=x,y,z)$. No strict physical law is the heart of such a description which means only the possibility to express the **P**(**E**) dependence in the form of a Taylor series

$$P_i = (dP_i/dE_k)E_k + (1/2)(d^2P_i/dE_k dE_l)E_l E_k + (1/6)(d^3P_i/dE_k dE_l dE_m)E_m E_l E_k + \cdots . \quad (1)$$

Here and below the Einstein summation convention is assumed. Traditionally, decomposition (1) is presented just as a sum of the linear, quadratic, and third-order parts:

$$P_i = P_i^{(1)} + P_i^{(2)} + P_i^{(3)} = \epsilon_0(\chi_{ik}^{(1)}E_k + \chi_{ikl}^{(2)}E_k E_l + \chi_{iklm}^{(3)}E_k E_l E_m), \quad (2)$$

where ϵ_0 is the permittivity of vacuum. The tensor coefficients $\chi_{ik}^{(1)}$ are defined as linear dielectric susceptibilities, and the quadratic and third-order susceptibilities are determined by coefficients $\chi_{ikl}^{(2)}$ and $\chi_{iklm}^{(3)}$.

The isotropy of bulk glass implies that its $\chi_{ikl}^{(2)}$ coefficients are equal to zero, and imposes the following constraints upon the $\chi_{ik}^{(1)}$ and $\chi_{iklm}^{(3)}$ components:[7]

$$\chi_{xx}^{(1)} = \chi_{yy}^{(1)} = \chi_{zz}^{(1)},$$

$$\chi_{xxxx}^{(3)} = \chi_{yyyy}^{(3)} = \chi_{zzzz}^{(3)},$$

$$\chi_{xxyy}^{(3)} = \chi_{xyyx}^{(3)} = \chi_{xyxy}^{(3)},$$

$$\chi_{xxxx}^{(3)} = \chi_{xxyy}^{(3)} + \chi_{xyyx}^{(3)} + \chi_{xyxy}^{(3)} = 3\chi_{xxyy}^{(3)}. \quad (3)$$

The NLO characteristics of glasses are frequently represented by the values $\chi_{xxxx}^{(3)}$ which will be referred to below as the third-order NLO susceptibility denoted as $\chi^{(3)}$. In practice, the linear susceptibility $\chi^{(1)}$ and the third-order NLO susceptibility $\chi^{(3)}$ can be evaluated (see Ref. 7) as follows (here and below the international unit system SI is used):

$$\chi^{(1)} = n_0^2 - 1, \quad (4)$$

$$\chi^{(3)} = 2n_2 n_0^2 c\epsilon_0/3, \quad (5)$$

where c is the light velocity, and n_0 and n_2 are the linear and nonlinear refractive indices, respectively, describing the relation between the refractive index n and the light intensity I:

$$n = n_0 + n_2 I. \quad (6)$$

The data on linear and NLO characteristics of TeO_2-based glasses are obtained by employing various experimental techniques, and are scattered in a number of publications using different unit systems in presenting the results. To make our analysis of these data as self-consistent as possible, they are assembled in Table I by using Eqs. (4) and (5) jointly with the relation

$$\chi^{(3)}(\mathrm{SI})/\chi^{(3)}(\mathrm{esu}) = 4\pi/(10^{-4}c)^2$$

borrowed from Ref. 18.

Table I shows that the linear indices n_0 measured in the wavelength interval between 840 and 1900 nm vary by about 10% with respect to its average value (which is close to n_0 of pure TeO_2 glass equal[8] to 2.11). Theoretically, this fact can be explained by frequency dispersion, described (see Ref. 12) as

$$\frac{\chi^{(1)}(\omega)}{\chi^{(1)}(0)} = \left(1 - \frac{\omega^2}{\omega_0^2}\right)^{-1} \quad (7)$$

with ω_0 determining the value of the bonding-antibonding energy gap $E_s = \hbar\omega_0$.

In fact, Eq. (7) gives an account of a lowest-order frequency response for a two-level system with an unperturbed energy splitting E_s. In optics, the relation given by Eq. (7) (written in the energy scale) is referred to as Sellmeier dispersion with the E_s parameter denoted as the electronic Sellmeier energy. As a rule, it adequately describes the relevant experimental evidence in the area of normal dispersion ($\omega \ll \omega_0$).

For tellurite glasses, the E_s value is evaluated[8] as being near 6.6 eV ($\omega_0 = 1.6\times10^{16}$ Hz) corresponding to the light wavelengths λ_0 of 190 nm. By using that value, Eq. (7) predicts a $\chi^{(1)}(\omega)/\chi^{(1)}(0)$ magnitude variation of about 1–5 % within the light wavelength interval between 1900 and 840 nm, which is a good correspondence with the behavior of the experimental values of $\chi^{(1)}$ in Table I. On the one hand, this fact indicates the physical meaningfulness of the

TABLE I. Experimental data on refractive indices and NLO characteristics of TeO_2-based glasses.

Percentage and type of modifier oxide	n_0	n_2 (10^{-19} m^2/W)	$\chi^{(3)}$ (10^{-21} m^2/V^2)	$\chi^{(3)}$ (10^{-13} esu)	λ (nm)	Reference
TeO_2 pure	2.11	24.72	19.68	**14.10**[a]	1900	8
$7.5Li_2O$	2.07	23.58	17.88	**12.81**		9
$20Li_2O$	1.98	11.75	8.18	**5.86**		
$25Li_2O$	1.94	8.79	5.88	**4.21**		
$5Na_2O$	2.07	13.43	10.14	**7.26**		
$10Na_2O$	2.02	11.33	8.18	**5.86**	1900	
$20Na_2O$	1.94	10.13	6.73	**4.82**		
$7.5K_2O$	2.03	13.94	10.21	**7.31**		
$15K_2O$	1.93	10.87	7.19	**5.15**		
$20K_2O$	1.88	8.47	5.28	**3.78**		
$5Nb_2O_5$	**2.23**	21.00	18.48	13.24	840	4
$10Nb_2O_5$	**2.24**	18.50	16.43	11.77		
$15Nb_2O_5$	**2.22**	18.10	15.79	11.31		
$20Nb_2O_5$	**2.26**	18.00	16.27	11.66		
$10Al_2O_3$	**2.04**	17.40	12.82	9.18		10
$15Al_2O_3$	**1.96**	11.80	8.02	5.75	840	
$20Al_2O_3$	**1.93**	10.90	7.19	5.15		
$10Al_2O_3$	**2.03**	5.38	3.92	2.81		6
$10Nb_2O_5$	**2.14**	6.93	5.64	4.04		
$15Nb_2O_5$	**2.15**	6.41	5.22	3.74		
$20Nb_2O_5$	**2.16**	5.94	4.88	3.50	1500	
$18Tl_2O$	**2.13**	8.60	6.87	4.92		
$21Tl_2O$	**2.09**	8.90	6.91	4.95		
$13.5Tl_2O$-$1.5Bi_2O_3$	**2.16**	9.10	7.49	5.36		
$10LaO_{1.5}$	2.11	2.10	1.66	**1.19**		3(a)
$15LaO_{1.5}$	2.10	1.96	1.54	**1.10**	1900	
$20LaO_{1.5}$	2.09	1.87	1.45	**1.04**		
$20Nb_2O_5$-10PbO				**1.4**	532	11
$20Nb_2O_5$				**7.2**		
$6TiO_2$-$2Li_2O$				**8**		
$20Nb_2O_5$-2.5ZnO				**8.2**		

[a]Figures printed in bold correspond to original data given in the cited papers.

approximation presented by Eq. (7); on the other hand, it can be thought that the linear optical characteristics in Table I (combined with energy and structural data) would provide an objective estimation of the accuracy of the quantum-chemical calculations used in this paper. We note that the coefficient n_0 of pure TeO_2 glass equal[8] to 2.11 exceeds noticeably (but not dramatically) that of pure SiO_2 glass equal to 1.44.[8]

Let us focus now on the NLO properties. To the best of our knowledge, no systematic measurements of the $\chi^{(3)}$ coefficients were reported, and the scattered data collected in Table I differ dramatically even for glasses having the same composition. We wish to underline that such inconsistencies in the measured values cannot be explained by the frequency dispersion effect. To argue this, the two-level perturbation theory[14] can be used providing the following frequency dispersion of the nonlinear susceptibility $\chi^{(3)}$:

$$\frac{\chi^{(3)}(\omega)}{\chi^{(3)}(0)} = \left(1 - \frac{\omega^2}{\omega_0^2}\right)^{-4} \tag{8}$$

We would like to point out that this general expression is remarkably in agreement with the frequency dependence of third-order NLO coefficients estimated from the *ab initio* calculations of the $Te(OH)_4$ cluster.[19]

Being used with $\omega_0 = 1.6 \times 10^{16}$ Hz, this predicts that the $\chi^{(3)}(\omega)$ values should monotonically increase in the proportion 1.07:1.25:1.72 for light beams having wavelengths equal to 1500, 840, and 532 nm, respectively. It is not clear which physical factor could be used to explain why the relevant experimental $\chi^{(3)}(\omega)$ values vary nonmonotonically (3.50:11.66:7.20), as the data of Table I (for the glass with 20% of Nb_2O_5 taken from Refs. 6, 4, and 11) show. At the same time, it is important that Eq. (8) shows that the $\chi^{(3)}(\omega)$ hypersusceptibilities of the TeO_2-based glass mea-

sured for λ equal to 1900 and 1500 nm differ from the static nonlinear susceptibility $\chi^{(3)}(0)$ by about 4–7 % only. This suggests that a static approximation can provide a quite adequate estimation of the hypersusceptibilities of TeO_2-based glass manifested for sufficiently long waves.

Although the data on NLO properties of different glasses represented in Table I are not self-consistent, nevertheless, they always manifest the same tendency, namely, the NLO coefficients of the $(100-x)TeO_2+xM_iO_j$ glasses increase with decreasing modifier concentration. (Rare exceptions, e.g., Refs. 3 and 5, which extend to glasses with modifiers involving cations with extremely high polarizability are beyond our consideration.) Thus, concerning the glasses mentioned in Table I, pure TeO_2 glass would have the highest $\chi^{(3)}$ susceptibility. Naturally, the knowledge of its experimental value is of importance for our study. The result of Ref. 7 seems to provide this (see Table I). However, we venture the opinion that it will be risky to consider this result noncritically without taking into account the limiting values $\chi^{(3)}$ which can be estimated from Table I for various $(100-x)TeO_2+xM_iO_j$ glass systems at $x\rightarrow 0$.

Two groups can be distinguished among the authors of the works referred to in Table I. The first group is related to Refs. 3, 8, and 9. All the measurements in these works were performed for $\lambda=1900$ nm. The results of Ref. 7, providing the $\chi^{(3)}$ value of pure TeO_2 glass equal to 19.7×10^{-21} m^2/V^2, seem to be confirmed by the data of Ref. 8 obtained for the TeO_2—Li_2O system (in extrapolating the modifier quantity, to zero), but those obtained in Ref. 9 for TeO_2—Na_2O and TeO_2—K_2O systems give estimations two times lower, i.e., about 10×10^{-21} m^2/V^2.

The data of the second group[4,6,10] were obtained for $\lambda=840$ nm (Refs. 4 and 10) and for $\lambda=1500$ nm.[6] According to these data, the long-wave limit of the $\chi^{(3)}$ (TeO_2) value can be estimated at about 10×10^{-21} m^2/V^2.

Thus, the analysis of the experimental data on the $\chi^{(3)}$ susceptibility of the TeO_2-based glass allows us to state that the static limit of this value for pure TeO_2 glass should lie between 10×10^{-21} and 20×10^{-21} m^2/V^2. We believe that the first of these values is more reliable.

The experimental $\chi^{(3)}$ values of the SiO_2-based glass are scattered within the interval $(0.05-0.39)\times10^{-21}$ m^2/V^2.[8,20] Thus, a comparison of the experimental data for the TeO_2-based glass and the SiO_2-based glass shows beyond any doubt that the former possesses superior NLO properties. In particular, in analyzing a series of comparative studies using the same experimental techniques, the following relations can be found: $\chi^{(3)}(85TeO_2\text{-}13.5Tl_2O\text{-}Bi_2O_3):\chi^{(3)}\times(SF_{59})=2.65$ (Ref. 6), $\chi^{(3)}(90TeO_2\text{-}10Al_2O_3):\chi^{(3)}(SF_{59})=4.8$ (Ref. 10), $\chi^{(3)}(TeO_2):\chi^{(3)}(SiO_2)=50$ (Ref. 8). (SF_{59} is the notation for commercial lead silicate glass produced by Schott Glass Technologies.)

III. THEORETICAL SCHEME AND CALCULATIONS

The microscopic polarizability and hyperpolarizabilties of a molecule are defined as the coefficients in linear and nonlinear terms in the expansion [similar to that in Eq. (1)] of components of a molecular dipole μ induced by an electric field E acting on this molecule:

$$\mu_i=\alpha_{ik}E_k+\frac{1}{2}\beta_{ikl}E_lE_k+\frac{1}{6}\gamma_{iklm}E_mE_lE_k+\cdots. \tag{9}$$

To deduce a relationship between dielectric susceptibilities $\chi^{(1)}$ and $\chi^{(3)}$ of an isotropic material and their microscopic "sources," namely, linear polarizability α_{ik} and third-order hyperpolarizability γ_{iklm} of the molecules that form that material, the two following points should be taken into account.

First, the macroscopic polarization **P** should be presented through a sum of molecular dipole moments μ over all N molecules in volume V,

$$\mathbf{P}=\frac{\sum_\mu}{V},$$

which can be expressed as

$$\mathbf{P}=\frac{\mu_{av}}{V_m}, \tag{10}$$

where $\mu_{av}=\frac{1}{N}\Sigma\mu$ is the average dipole moment and $V_m=\frac{1}{N}V$ is the molecular volume (volume per one molecule).

In isotropic materials, the vector form of Eq. (10) can be replaced by a scalar representation by introducing the linear polarizability α averaged over possible molecular orientations and the averaged third-order hyperpolarizability γ defined in Ref. 21 as

$$\alpha=\frac{1}{3}(\alpha_{xx}+\alpha_{yy}+\alpha_{zz}), \tag{11}$$

$$\gamma=\frac{1}{5}(\gamma_{xxxx}+\gamma_{yyyy}+\gamma_{zzzzz}+2\gamma_{yyzz}+2\gamma_{xxzz}+2\gamma_{xxyy}). \tag{12}$$

After omitting in Eq. (9) the quadratic contribution to μ_{av} (which vanishes in isotropic materials), the orientationally averaged molecular dipole moment can be described in a scalar form as

$$\mu_{av}=\mu_{av}^{(1)}+\mu_{av}^{(3)}=\alpha E+\frac{1}{6}\gamma E^3. \tag{13}$$

Second, it should be taken into account that the macroscopic field E in Eqs. (1) and (2) is an external field toward the molecule, whereas the field E in Eqs. (9) and (13) must be specified as a microscopic internal field (including, apart from the macroscopic field, the contributions from the local molecular dipole moments). These two fields are interrelated as

$$E_{int}=E_{ext}f_L, \tag{14}$$

and the values in question can be presented in the form

$$\chi^{(1)}=\frac{1}{\epsilon_0 V_m}\alpha f_L \tag{15}$$

$$\chi^{(3)} = \frac{1}{6\epsilon_0 V_m}\gamma f_L^3 \tag{16}$$

where f_L is the Lorentz factor which in the case of an isotropic material is given by the expression

$$f_L = 1 + \frac{1}{3}\chi^{(1)} = \left(1 - \frac{\alpha}{3\epsilon_0 V_m}\right)^{-1} \tag{17}$$

Now the question arises: Which molecular clusters can be taken as models of the structural blocks of TeO_2 glass? Theoretically, it seems to be evident that the condensation of the TeO_2 polar molecules would pass through the formation of polymerized associations. These can also be found in the gaseous and liquid phases, and thus would be inherent in a glassy phase.

The results of a preliminary *ab initio* study showed that in the case of TeO_2, such associations can exist in the form of various $(TeO_2)_p$ polymer molecules.[16] The preliminary estimations of the NLO characteristics of TeO_2 glass deduced from the calculated third-order hyperpolarizabilities of those molecules provided quite promising results.[17]

In the present paper, we develop this approach and apply it to two groups of polymers: the $(TeO_2)_p$ molecules (with p varying up to 12), and the $(SiO_2)_p$ polymer molecules (with p up to 9). The comparative analysis of the results obtained allows us to offer a hypothesis concerning the peculiarities of the polarization mechanisms of TeO_2 and SiO_2 glasses which account for the dramatic difference in their NLO properties.

As a computational *ab initio* method, the density functional theory realized in Beck's three-parameter hybrid method using the Lee-Yang-Parr correlation functional[22] (B3LYP) was chosen. This method, being run within the 3-21G** basis set by the GAUSSIAN program,[23] was found to be capable of reproducing satisfactorily the energies, geometries, and vibrational spectra of many-electron systems such as molecules containing several tellurium atoms. The efficiency of this method was confirmed in preceding studies of tellurium oxide[16,17,24,25] and silicon oxide[26,27] molecules.

During the calculations, the static polarizability tensor α_{ik} was first computed analytically for every $(XO_2)_p$ molecule (X=Si, Te), and then the third-order hyperpolarizability tensor $\gamma_{ijkl} = \frac{d^2\alpha_{ij}}{dE_k dE_l}$ was deduced by numerical differentiation with respect to the static electric field E.

The volume V_m of the molecules was evaluated as

$$V_m = pV_s \quad \text{with } V_s = M/d, \tag{18}$$

where M is the mass of the XO_2 formula unit, d is the relevant glass density, and the V_s value can be specified as the specific volume of the XO_2 unit in the molecule.

Now, from a joint consideration of Eqs. (15)–(18), the final forms of the relations for $\chi^{(1)}$ and $\chi^{(3)}$ are

$$\chi^{(1)} = \frac{\alpha_s}{\epsilon_0 V_s}\left(1 - \frac{\alpha_s}{3\epsilon_0 V_s}\right)^{-1}, \tag{19}$$

$$\chi^{(3)} = \frac{\gamma_s}{6\epsilon_0 V_s}\left(1 - \frac{\alpha_s}{3\epsilon_0 V_s}\right)^{-3}, \tag{20}$$

with

$$\alpha_s = \alpha/p \quad \text{and} \quad \gamma_s = \gamma/p. \tag{21}$$

The values α_s and γ_s will be referred to below as the specific linear polarizability and specific third-order hyperpolarizability of a given polymer, respectively. By using the experimental data on the densities of SiO_2 glass[28] and of TeO_2 glass,[29] the values V_s=45.2 Å^3 and V_s=47.8 Å^3 were evaluated for the SiO_2 and TeO_2 glasses, respectively. In fact, they represented the constant parameters in Eqs. (19) and (20).

IV. RESULTS

A. Structures of SiO_2-based polymers

The calculations revealed a series of stable $(SiO_2)_p$ polymers with $p \leqslant 9$, the geometries of which were determined theoretically by energy optimization. A complete list of polymer molecules obtained in this way is represented in Table II. Some of the structures are shown in Fig. 1. It is seen that the polymerization of SiO_2 molecules includes the formation of SiO_4 tetrahedrons and SiO_3 groups interconnected by common edges or common corners. As a result, cycles built up of Si—O—Si bridges are formed. Among optimized molecular structures listed in Table II, one can distinguish such cycles with N bridges ($N \leqslant 6$). We use N_i to label different molecular structures. So the structure consisting of two three-membered cycles [Fig. 1(a)] is referred to as 3-3. Cycles surrounded by other cycles are labeled with N in parentheses. This is the case of the structure shown in Fig. 1(h) consisting of four three-membered cycles which is labeled as (3)-3-3-3. Another type of polymerization proceeds through formation of chains built up of edge-sharing SiO_4 tetrahedrons. One representative of this family is shown in Fig. 1(c). Formally, these chains can be considered as being part of two-membered cycles. Alternatively, such cycles can be referred to as double $Si\langle^{O}_{O}\rangle Si$ bridges.

The structure with p=8 shown in Fig. 1(g) was obtained by geometry optimization of the initial configuration formed by eight Si atoms in the corners of a cube and 12 O atoms in the middle of the edges. The residual four O atoms were attached to four Si atoms which form a tetrahedron. So the initial configuration was taken as a cube formed by four SiO_4 tetrahedrons and four SiO_3 pyramids interconnected by common corners. The optimized structure shown in Fig. 1(g) (and denoted as "cube" in Table II) retains the topology of the initial one, even if the O—Si—O angles have changed.

B. Structures of TeO_2-based polymers

The theoretical structures of the $(TeO_2)_p$ polymer molecules found by the *ab initio* calculations are many and varied.[16] They are partially shown in Fig. 2.

The diversity of the theoretical structures of the $(TeO_2)_p$ polymer molecules, found by the *ab initio* calculations, is larger. These structures have been discussed in a previous

TABLE II. Calculated energies E and polymerization energies E_p of the $(SiO_2)_p$ molecules.

p	Structure	E (a.u.)	E_p (kcal/mol)
1	Monomer	−437.6699456	0
2	Dimer	−875.5331947	−60.64718
3	Chain	−1313.4099058	−83.67967
3	3	−1313.4099058	−78.08477
4	Chain	−1751.2832817	−94.6727
4	4	−1751.2006107	−81.70348
4	3-2	−1751.2677067	−92.22933
5	Chain	−2189.1560578	−101.19324
5	5	−2189.0077327	−82.57814
5	4-2	−2189.0872497	−92.55769
5	3-3	−2189.1240394	−97.1787
6	Chain	−2627.0285724	−105.51292
6	6	−2626.8101738	−82.6717
6	(3)-2-2-2	−2627.0317486	−105.8451
6	4-3	−2626.9431579	−96.57984
6	(4)-2-2	−2626.9735322	−99.75654
6	(3)-3-2	−2627.007137	−103.2711
6	Octahedron	−2625.9050953	−92.59907
7	Chain	−3064.9012185	−108.61019
7	(3)-3-3	−3064.8630239	−105.18627
8	Chain	−3502.7733535	−110.89306
8	(3)-3-3-2	−3502.7443355	−108.61692
8	3-3-3-3	−3502.8999506	−120.82318
8	(4)-3-3	−3502.6854074	−103.99468
8	(4)-2-2-2-2	−3502.7378083	−108.10494
8	Cube	−3502.7400454	−108.28041
9	Chain	−3940.6460100	−112.70463
9	(3)-3-3-3-3	−3940.59996086	−109.46972

TABLE III. Calculated energies E and polymerization energies E_p of the $(TeO_2)_p$ molecules.

p	Type	E (a.u.)	E_p (kcal/mol)
1	Monomer	−6735.4944	0
2	Dimer	−13471.11126	−38.40989
3	Cycle	−20206.70641	−46.67608
3	Chain	−20206.71590	−48.66131
4	Cycle	−26942.27312	−46.34858
4	Chain	−26942.32435	−54.38485
4	Ring	−26942.38114	−63.29365
4	3D	−26942.38154	−63.3573
5	Chain	−33677.93296	−57.83845
5	Ring	−33678.01067	−67.59175
5	3D	−33677.94257	−59.0445
5	3D	−33677.98576	−64.46536
6	Cycle	−40413.42351	−47.79453
6	Chain	−40413.54096	−60.07795
6	Ring	−40413.61769	−68.10272
6	3D	−40413.40919	−46.29709
8	Chain	−53884.7548	−62.70719
8	Ring	−53884.80032	−66.27799
8	2×chain	−53884.74449	−61.89806
8	3D	−53884.80432	−66.59139
10	Chain	−67355.97038	−64.39353
12	Chain	−80827.18948	−65.70214
12	2×6	−80827.23397	−68.02887
12	3D	−80827.39577	−76.48986

paper.[16] Some examples are shown in Fig. 2 and the energies of all molecules are represented in Table III. From this figure it is seen that threefold- or fourfold-coordinated atoms of tellurium can be found in these structures. The threefold-coordinated Te atoms are in the apexes of the TeO_3 pyramids. As a rule, one bond of such a pyramid is terminal and the two others form the Te—O—Te bridges. As for the fourfold-coordinated Te atoms, their coordination polyhedrons are conventionally regarded as distorted trigonal bipyramids (TBPs) called bisphenoids. They contain two axial bonds (2.08–2.15 Å) which form an angle of the order of 160°–180°, and two equatorial bonds (1.89–1.96 Å) forming an angle about 100°.

Several structural types can be distinguished among the $(TeO_2)_p$ polymer molecules: (1) cycles formed by corner-sharing TeO_3 pyramids [Fig. 2(a)]; (2) chains formed by edge-sharing TBPs [Fig. 2(b)]; (3) rings formed by self-switching of these chains [Fig. 2(c)].

Various combined structures can be obtained by association of the above listed basic structures. For example, crossing of two chains leads to formation of a quasiplanar structures [Fig. 2(e)]. Another example, assemblage of several rings or cycles, produces formation of tubes [Figs. 2(g)].

The diversity of the telluria polymer structures comes from two basic reasons—the variability of the coordination number of the Te atoms and the rather particular shape of the TeO_4 polyhedron. The latter circumstance gives rise to the existence of rather particular polymer molecules—spherelike three-dimensional (3D) framework structures such as those shown in Figs. 2(d), 2(h), and 2(f).

C. Energies of the $(SiO_2)_p$ and $(TeO_2)_p$ polymers

To analyze the relative stability of various polymers, the polymerization energies, defined by the relation

$$E_p = \frac{1}{p}\{E[(XO_2)_p] - pE(XO_2)\}, \tag{22}$$

were calculated for all the molecules under study. Figures 3(a) and 3(d) show unequivocally that the E_p values decrease at increasing p. Their $p \to \infty$ limits can be estimated as lying near −120 kcal/mol for $(SiO_2)_p$, and near −75 kcal/mol for $(TeO_2)_p$. According to Eq. (13), they can be considered as the heat of sublimation of the XO_2 molecules from the solid phase. The relevant experimental data show 141 kcal/mol for X=Si (Ref. 30) and 69 kcal/mol for X=Te.[31] The good agreement between theory and experiment counts in favor of the adopted computational routine.

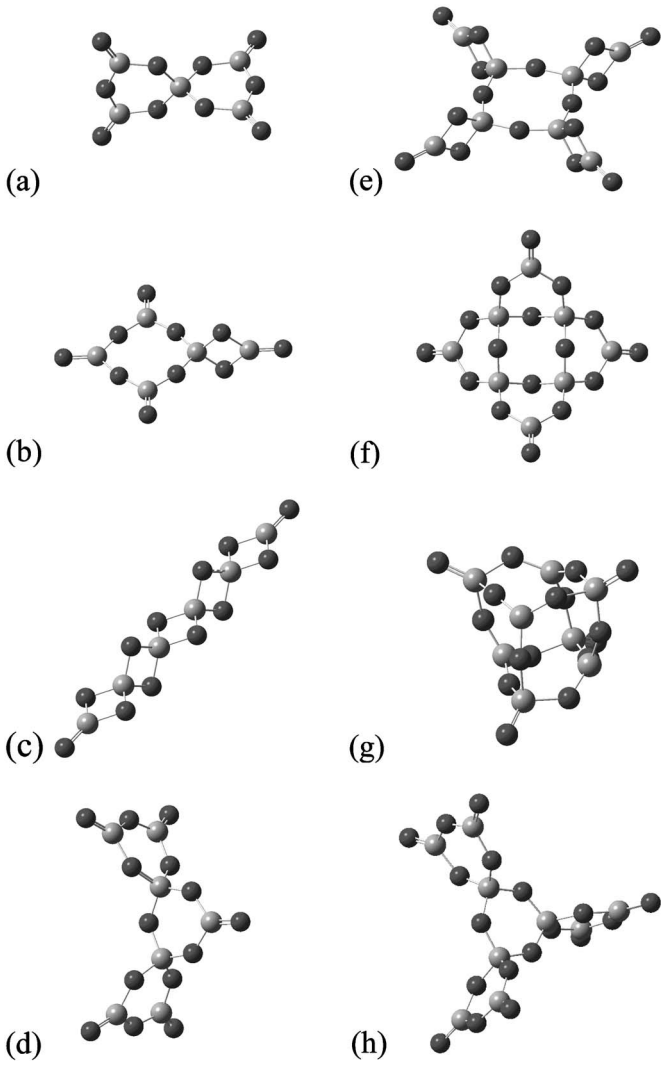

FIG. 1. Structures of polymer molecules $(SiO_2)_p$ obtained by *ab initio* calculations: (a) 3-3, $p=5$; (b) 4-2, $p=5$; (c) chain, $p=6$; (d) 3-3-3, $p=7$; (e) (4)-2-2-2, $p=8$; (f) 3-3-3-3, $p=8$; (g) cube, $p=8$; (h) (3)-3-3-3, $p=9$.

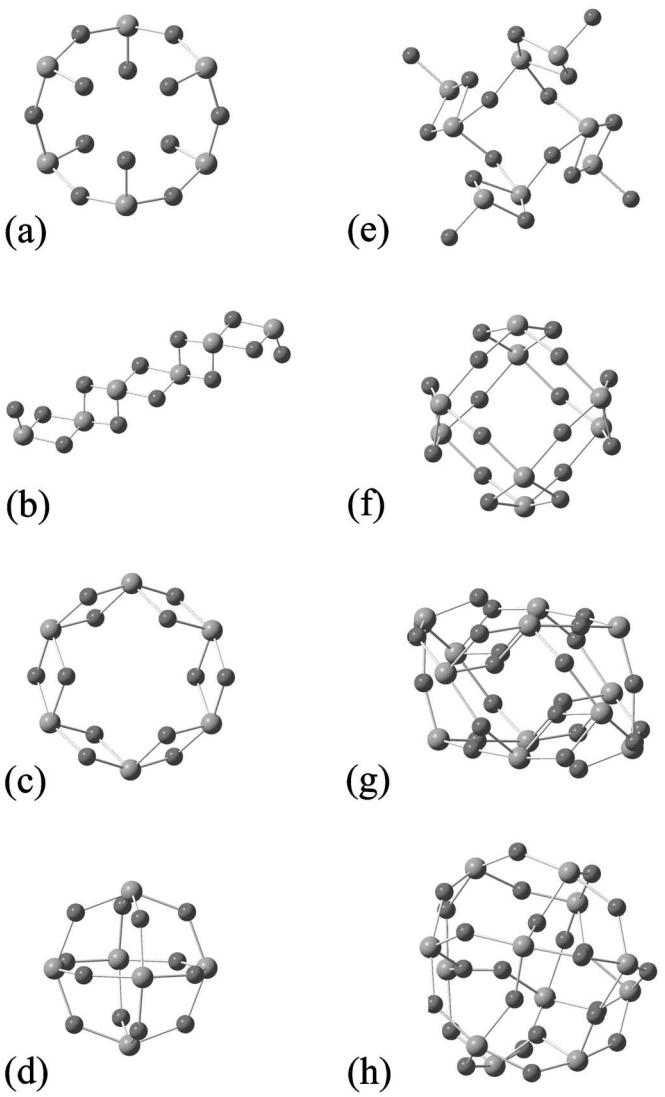

FIG. 2. Structures of polymer molecules $(TeO_2)_p$ obtained by *ab initio* calculations: (a) cycle, $p=6$; (b) chain, $p=6$; (c) ring, $p=6$; (d) octahedron, $p=6$; (e) crossing of two four-membered chains, $p=8$; (f) 3D structure, $p=8$; (g) agglomeration of two six-membered cycles, $p=12$; (h) 3D structure, $p=12$.

D. Linear refractive indices

The polarizability tensors of the $(SiO_2)_p$ and $(TeO_2)_p$ molecules listed in Tables II and III were calculated. These values were used to evaluate [via Eqs. (4), (11), and (19)] the n_0 indices of SiO_2 and TeO_2 glass by considering these molecules as basic structural units of those glasses. The n_0 values thus obtained are presented in Figs. 3(b) and 3(e) in dependence on the p value.

Figure 3(e) shows that the simulated $n_0(p)$ values for SiO_2 glass show no systematic dependence on the p number: the $n_0(p)$ values are scattered in the narrow interval between 1.40 and 1.46 (n_0 for $p=1$ has no sense), being close to the experimental value $n_0=1.44$.[8]

In contrast to this, the n_0 indices evaluated from the polarizabilities of the $(TeO_2)_p$ molecules increase with p. This is most pronounced in the series of linear chain molecules, the contributions of which are shown by crosses in Figs. 3(a)–3(c). For these molecules the calculated $n_0(p)$ systematically increases with p, so that its limit at $p\rightarrow\infty$ practically coincides with the experimental value 2.11.[8] It shows that the cluster approach can provide quite realistic results when simulating glassy state properties. At the same time, estimations made for the rest of the $(TeO_2)_p$ clusters seem to have no regular behavior and stay below 2.0.

E. Nonlinear susceptibility

The calculated third-order hyperpolarizabilities of the $(XO_2)_p$ molecules were used to simulate the $\chi^{(3)}$ values of the glass under consideration [via Eq. (20)], and the resulting $\chi^{(3)}(p)$ dependencies are shown in Figs. 3(c) and 3(f).

It is seen that the $\chi^{(3)}(p)$ values calculated for SiO_2 glass [Fig. 3(f)] show no definitive trend with increasing p and are scattered in the interval between 0.05 and 0.20 (10^{-21} m^2/V^2) (the case $p=1$ has no sense). Note that the

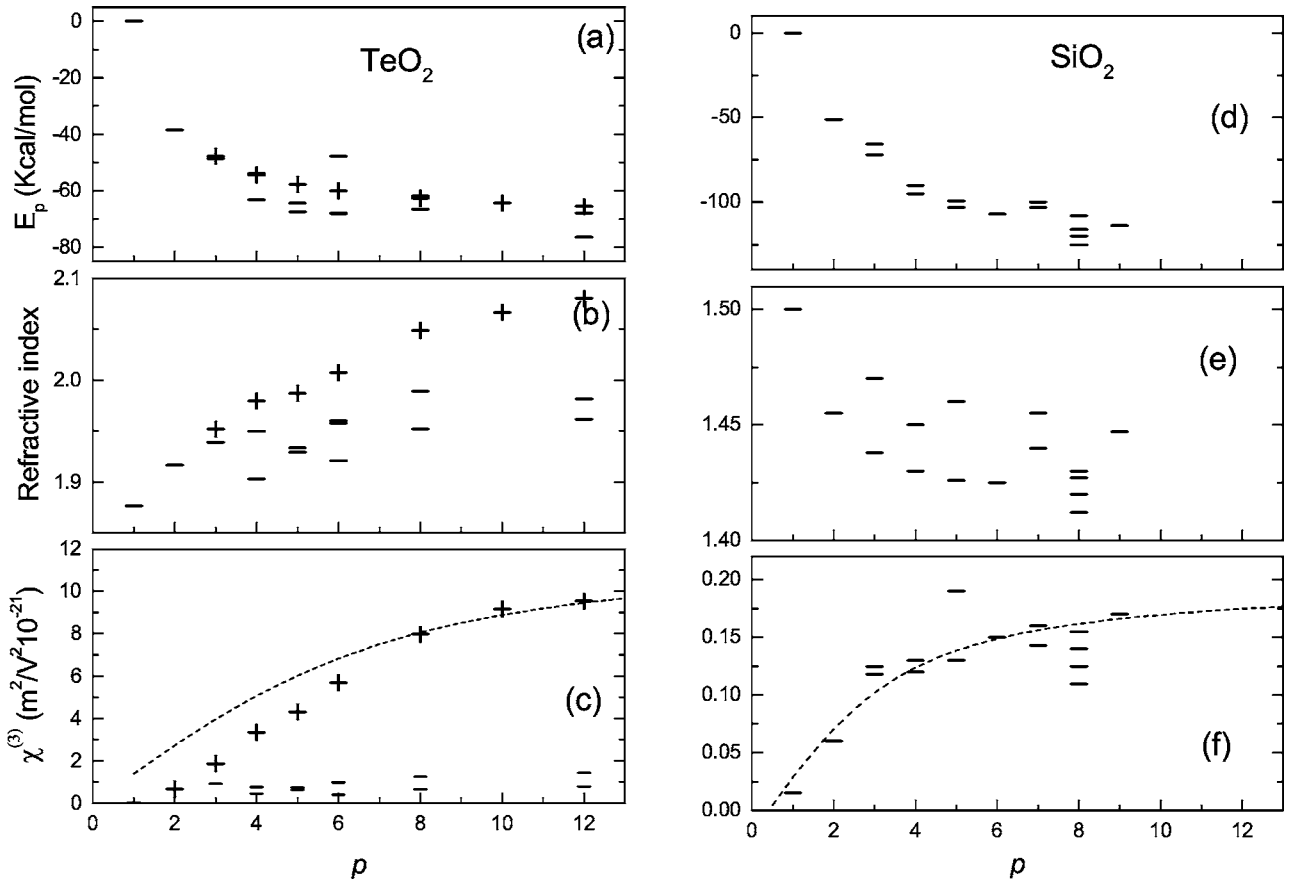

FIG. 3. Energies of formation (a),(d), refractive indices (b),(e), and third-order susceptibilities (c),(f) of TeO_2 (left panels) and SiO_2 (right panels) glasses estimated from calculated characteristics of $(TeO_2)_p$ and $(SiO_2)_p$ molecules in dependence on the polymerization number p.

two experimental estimations of the $\chi^{(3)}$ for SiO_2 glass are conflicting: 0.05 (Ref. 20) and 0.39 (10^{-21} m^2/V^2).[8]

As to the $\chi^{(3)}$ values calculated for TeO_2 glass [Fig. 3(c)], it is remarkable that they show a peculiarity similar to that observed in Fig. 3(e). Actually, the $\chi^{(3)}$ values related to the $(TeO_2)_p$ chains show a regular and strongly pronounced increase tending to 10×10^{-21} m^2/V^2 at $p\rightarrow\infty$, which is in dramatic contrast with the properties of the other $(TeO_2)_p$ structures presented in Fig. 2.

V. DISCUSSION AND HYPOTHESIS

A. $(SiO_2)_p$ structures

The simulated structures of the $(SiO_2)_p$ polymer molecules (see Fig. 1) allow the suggestion that the elementary structural subunits of glassy SiO_2 are rings formed by two, three, four, etc., Si—O—Si bridges. Similar subunits have been found in Refs. 32 and 33. Linkage of such rings leads to formation of a 3D framework. This proceeds through association of two terminal Si═O bonds in one $Si\langle^{O}_{O}\rangle Si$ double bridge or by association of three terminal Si═O bonds in a three-membered Si—O—Si ring, etc. On the contrary, the molecules in Fig. 1 can be considered as subunits coming from breaking of Si—O—Si bridges in a SiO_2 framework. So the threefold-coordinated Si atoms with one terminal Si═O bond represent possible point defects of the SiO_2 framework resulting from ablation of one link of a Si—O—Si ring.

Let us discuss the correlations between calculated polymerization energies (collected in Table II) and molecular structure.

First of all it can be noted that the lowest polymerization energy is inherent to the structure with the least content of terminal Si═O bonds. This explains why at any p value the planar cycle polymers (with p terminal bonds) have the highest energies and the chain polymers (with two terminal bonds) have rather low energies.

Second, it is seen that the three-membered and four-membered cycles are energetically more preferable than the two-membered ones. This can be illustrated by comparing the molecule 3-3 [Fig. 1(a)] with 4-2 [Fig. 1(b)] and the molecule (4)-2-2-2-2 [Fig. 1(e)] with 3-3-3-3 [Fig. 1(f)]. Furthermore, this rule allows one to explain why the chain polymers, even if they have only two terminal bonds, are not the ground-state structures for $p>6$. Note that presence of the two-membered cycles (or the double bridges $Si\langle^{O}_{O}\rangle Si$) denotes corner sharing between two SiO_4 or SiO_3 units. The calculated energies confirm that the corner sharing (i.e., formation of the Si—O—Si single bridges) is preferable to edge sharing.

The relatively high energy of terminal bonds fosters understanding of the high polymerization ability inherent to condensed silica: two molecules with terminal bonds easily

link together by forming a $Si\langle{}^{O}_{O}\rangle Si$ double bridge. And the relatively high energy of these double bridges favors further polymerization: such a bridge coming together with a terminal Si═O bond results in formation of a three-membered cycle.

To summarize, our results confirm the structural model of vitreous silica as an ensemble of corner-sharing SiO_4 tetrahedrons forming cycles with various numbers of Si—O—Si bridges ($p>2$). The $Si\langle{}^{O}_{O}\rangle Si$ double bridges and the SiO_3 units with one terminal Si═O bond can be considered as possible defect structures.

Another possible type of point defect is represented by the Si_8O_{16} molecule shown in Fig. 1(g). This molecular structure involves four SiO_3 pyramids with three bridging bonds and four SiO_4 tetrahedrons with one terminal bond. Similar subunits have been discussed as possible point defects in silicate glasses.[34] Calculated energies (see Table II) give evidence that the stability of this molecule is the lowest one among other $(SiO_2)_8$ polymers [e.g., those shown in Figs. 1(e) and 1(f)]. Nevertheless, this structure provides us a good example for discussing the formation of a condensed phase from molecular species. From the point of view of the "packing criterion" the cluster shown in Fig 1(g) can be distinguished as the most realistic structural fragment affording the formation of the "ideal" SiO_2 framework. Actually, an ensemble of such clusters would always contain a number of terminal Si—O bonds equal to the number of the SiO_3 pyramids, which is necessary for the polymerization of the clusters into a 3D structure in which all oxygen atoms would be involved in the Si—O—Si bridges, and consequently all silicon atoms would be centers of SiO_4 tetrahedrons.

B. $(TeO_2)_p$ structures

The calculations reveal a large variety of different types of $(TeO_2)_p$ clusters. They were classified in Sec. IV B and are partially shown in Fig. 2. The calculated energies (see Table III) allow us to estimate the relative stability of different types of polymers. The same main tendencies [as those discussed in the preceding section for $(SiO_2)_p$ molecules] can be noted for $(TeO_2)_p$ molecules. Te═O terminal bonds are the least energetically favorable; Te—O—Te single bridges are preferable to $Te\langle{}^{O}_{O}\rangle Te$ double bridges and TeO_4 units to TeO_3 units. As a result, cycles [such as that shown in Fig. 2(a)] have the highest energies; rings [as shown in Fig. 2(c)] are preferable to chains [like that shown in Fig. 2(b)]; structures including neither Te═O terminal bonds, nor TeO_3 units, nor the $Te\langle{}^{O}_{O}\rangle Te$ double bridges [Fig. 2(g)] have the lowest polymerization energy. Hence, the calculations confirm that the most stable structure of telluria polymers should be an ensemble of corner-sharing TeO_4 units. Other structural units (such as Te═O terminal bonds, TeO_3 units, and $Te\langle{}^{O}_{O}\rangle Te$ double bridges) can be considered as local defect structures.

As in silica polymers, the presence of terminal bonds in a $(TeO_2)_p$ molecule augments its E_p energy significantly. Comparison of energies of ring structures [like that shown in Fig. 2(c)] and chain structures [such as shown in Fig. 2(b)] allows us to estimate energy of formation of the $Te\langle{}^{O}_{O}\rangle Te$ double bridge from two terminal Te═O bonds at about 5 kcal/mol. At the same time, in contrast to the silica polymers, the difference between E_p energies of the structures built up of $Te\langle{}^{O}_{O}\rangle Te$ double bridges and Te—O—Te single bridges is not too significant. This can be illustrated by comparing the energies of two polymers at $p=8$: the ring structure and the 3D structure shown in Fig. 2(f). All oxygen atoms in the former structure belong to the $Te\langle{}^{O}_{O}\rangle Te$ double bridges, whereas in the latter structure these contain only half of them and the rest belong to the Te—O—Te single bridges. The results presented in Table III show that the polymerization energies of these structures differ only by 0.5%. Indeed, in contrast to the silica, the $Te\langle{}^{O}_{O}\rangle Te$ double bridges have been found experimentally in various tellurite crystals as well as in the β-TeO_2.[35] This allows to suggest that the polymer structures which contain the $Te\langle{}^{O}_{O}\rangle Te$ double bridges can abundantly occur in the structure of glassy TeO_2. In particular, this is valid for chain structures. It should be emphasized that only this family of $(TeO_2)_p$ polymers shows rather high polarizability and hyperpolarizability values, which can provide a correspondence between calculated and measured dielectric characteristics of TeO_2 glass.

C. Linear susceptibility

It follows from Figs. 3(b) and 3(e) that the calculations correctly reproduce experimental linear refractive indices both for SiO_2 and TeO_2 glass (1.44 and 2.11, respectively). At the same time, Figs. 3(b) and 3(e) show that most of the clusters manifest no noticeable variations of the calculated n_0 values. Therefore it can be concluded that the specific linear polarizability of these fragments is practically independent of their form and size, which can indicate that its mechanism is essentially localized. The only exception is the linear polarizability of the chainlike $(TeO_2)_p$ molecules which slightly but clearly increases at increasing p. This fact can be interpreted as a manifestation of nonlocal effects in the electron distribution response in such structures.

D. Nonlinear susceptibility $\chi^{(3)}$

First of all, note that for a given type of $(XO_2)_p$ polymer, the dependence of the relevant $\chi^{(3)}$ values on the number p is determined by the behavior of the specific third-order hyperpolarizability γ_s only if the specific linear polarizability α_s does not show strong p dependence [see Eq. (20)].

Figure 3(f) shows that the specific third-order hyperpolarizability of the $(SiO_2)_p$ molecules increases for $p=1,2,3$, but from $p=5$ onward its average values are practically constant. This fact evidences the nonlocal nature of the third-order hyperpolarizability in the studied molecules, suggesting that the domain of this nonlocality in the $(SiO_2)_p$ polymers covers 3–4 SiO_2 units.

A similar effect, but in a much more impressive form, can clearly be seen in Fig. 3(c). Actually, with increasing p, the $\chi^{(3)}(p)$ values deduced for the model of TeO_2 glass "made" of the $(TeO_2)_p$ chains manifest a huge increase from 1×10^{-21} up to 10×10^{-21} m^2/V^2, thus achieving the experimental value of this coefficient. This fact stands out sharply

against a much weaker and poorly understandable tendency manifested by the $\chi^{(3)}$ coefficients related to the rest of TeO_2-based clusters having such characteristics hardly achieving 1×10^{-21} m^2/V^2. Thus it can be repeatedly stated that the experimental hypersusceptibility of glassy TeO_2 can be realistically reproduced by the properties inherent for $(TeO_2)_p$ chains only.

We would like to emphasize that the latter point argues in favor of the two hypotheses that (1) TeO_2 glass is mainly made of $(TeO_2)_p$ chains; and (2) the exceptional third-order hypersusceptibility of this glass is determined by a strong nonlocality of the electron distribution response within these chains.

It follows from the first hypothesis that the formation of the 3D framework from these chains would occur through breaking of $Te\langle{}^{O}_{O}\rangle Te$ double bridges and creation of the interchain Te—O—Te bridges, thus resulting in a structure in which the main structural blocks are organized in the same way as those in the γ-TeO_2 lattice.[36] This is supported by the fact that the first phase appearing during the crystallization of pure TeO_2 glass is the γ-TeO_2 lattice.

The second hypothesis can be discussed with more details by using the ideas of the theory of nonlocal polarizability (see Ref. 37 and references therein) which consider polarizatiom properties of an extended system in terms of the spatial dipole moment distribution $\mu(x)$ and implies that the electric field, being applied at point x, would induce a dipole moment not only at the very point x but in the vicinity of this point. Therefore, the distribution of the third-order dipole moment induced by a electric field $E(x)$ can be expressed as

$$\mu^{(3)}(x)=\frac{1}{6}\int g(x,x')E^3(x')dx', \tag{23}$$

where $g(x,x')$ is a nonlocal third-order polarizability function. Below we shall consider the case of homogeneous linear chain polymers formed from p identical links. The homogeneity of a chain implies that $g(x,x')=g(x-x')$.[37] In this case, a uniform electric field E acting on the chain consisting of p links would induce the dipole moment in which the third-order part can be described by an expression

$$\mu^{(3)}=\int \mu^{(3)}(x)dx=\frac{1}{6}E^3\int_{-p/2}^{p/2}dx\int_{-p/2}^{p/2}g(x-x')dx', \tag{24}$$

where x values are implied to be given in units of the link length. To rationalize the form of the $g(x-x')$ function, we use a Gaussian shaped approximation:

$$g(x-x')=G\exp\left[-\left(\frac{x-x'}{\sigma}\right)^2\right], \tag{25}$$

in which the parameter σ specifies a characteristic length of the dielectric response. This means that the function $g(x-x')$ rapidly vanishes if $|x-x'|>\sigma$.

Putting Eq. (25) in Eq. (24) and taking into account Eqs. (13) and (21), we can express the specific third-order hyperpolarizability γ_s of the chain as follows:

$$\gamma_s(p)=\frac{G}{p}\int_{-p/2}^{p/2}dx\int_{-p/2}^{p/2}\exp\left[-\left(\frac{x-x'}{\sigma}\right)^2\right]dx'. \tag{26}$$

According to Eq. (20) this value would completely determine the variation of $\chi^{(3)}$ at increasing number p if the specific linear polarizability α_s shows no p dependence. It can be concluded from Fig. 3(b) that this condition is satisfied with accuracy by 10% for $(TeO_2)_p$ polymers. We find this more than sufficient.

Consequently, the parameters G and σ in Eq. (26) can be varied to fit the relevant $\gamma_s(p)$ to the $\chi^{(3)}(p)$ values marked by crosses in Fig. 3(c). The same operation can be done to reproduce the position of the bars in Fig. 3(f). The results of such procedures are shown by dashed lines in both of these figures. The σ value thus found was $\sigma=10$ for the $(TeO_2)_p$ polymers and $\sigma=5$ for the $(SiO_2)_p$ polymers. We interpret this as an indication that the nonlinear dielectric response is much more delocalized in the TeO_2-based structures, being extended up to ten linked polyhedrons.

E. Modifier effect on the NLO properties of tellurite glasses

To clarify why NLO coefficients of tellurite structures decrease as a rule, along with increasing quantity of a modifier, the above model was used. First remember, that a "classic" (ortho)tellurite is a compound which can be classified as a salt of the tellurous acid H_2TeO_3,

$$nM+pH_2TeO_3=pH_2+M_nTe_pO_{3p}, \tag{27}$$

in which the complex anion is made of elementary bricks—pyramidlike $[TeO_3]^{2-}$ orthoanions. In practice, the tellurites are synthesized during the reaction between TeO_2 and a modifier oxide

$$pTeO_2+nM_kO_j=M_{nk}Te_pO_{2p+y}, \tag{28}$$

where $y=nj$. Normally, reaction (28) passes in a liquid phase in which the telluria component is present in the form of molecules TeO_2, and the modifier one is dissociated into O^{2-} and $M^{2j/k}$ ions. If the number of oxygen O^{2-} is sufficient to transform all the TeO_2 molecules into $[TeO_3]^{2-}$ units (i.e., $y=p$), the anionic system of the tellurite will consist of these units only. If this is not the case, (i.e., $y<p$), the complex anion $[Te_pO_{2p+y}]^{2y-}$ will be made of y pyramids TeO_3 mixed with $p-y$ molecules TeO_2. In crystalline structures, such anions very frequently have chainlike structures. Thus, by varying the y value from 0 to p in Eq. (28), all the TeO_2-based compounds between two limiting cases, pure TeO_2 and orthotellurite $M_{nk}(TeO_3)_p$, can be listed. Assuming that pure TeO_2 is made of $(TeO_2)_p$ infinite chains [i.e., of $[Te_pO_{2p+y}]^{2y-}$ chains with $y=0$ and $p\rightarrow\infty$], whereas the $M_{nk}(TeO_3)_p$ orthotellurite is made of TeO_3 chains consisting of one link only ($y=1$; $p=1$), we may believe that all the intermediate structures would contain complex anions in the form of $[Te_pO_{2p+y}]^{2y-}$ chains, the length of which (expressed as the number p) would diminish from $p=\infty$ to $p=1$ at an increasing modifier quantity from $n=0$ to $n=j/p$. Strictly speaking, no direct evidence indicates that this is the case for tellurite glasses, but chainlike $[Te_pO_{2p+y}]^{2y-}$ anions with

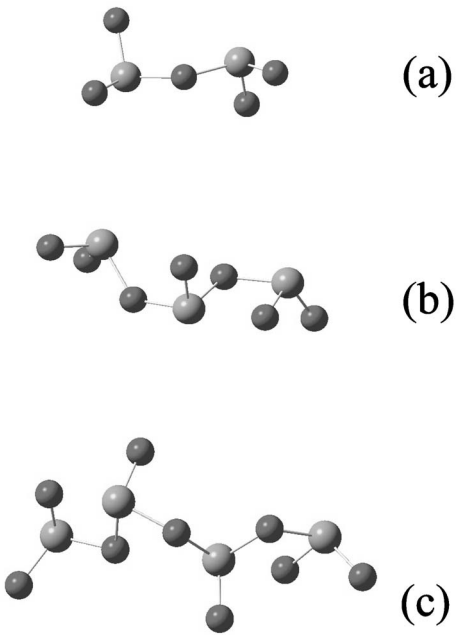

FIG. 4. Structure of the chain anions $[Te_2O_5]^{2-}$ (a), $[Te_3O_7]^{2-}$ (b), and $[Te_4O_9]^{2-}$ (c) established by DFT energy optimization.

$p=2-4$ and $y=1-2$ have been found as the typical structural fragments of crystalline tellurites (see, e.g., Ref. 38). It can be thought that they can exist in the glass as well.

Below we restrict our consideration to the case $y=1$, i.e., the case of the cations M^+ In this case the chemical formula of the tellurite anions in Eq. (28) is expressed as $[Te_pO_{2p+1}]^{2-}$ and Eq. (28) can be rewritten as an equation of reaction of x moles of the alkaline oxide M_2O and $100-x$ moles of telluria:

$$(100-x)TeO_2 + xM_2O = xM_2Te_{(100-x)/x}O_{2(100-x)/x+1}. \tag{29}$$

In comparing the right-hand sides of Eqs. (28) and (29), the number p (which determines the chain length) can be expressed as a function of the composition parameter x:

$$p(x) = (100-x)/x. \tag{30}$$

Therefore, according to this hypothesis, the compositions (29) with $x=33.3$, 25, and 20 would contain chainlike tellurite anions $[Te_pO_{2p+1}]^{2-}$ with $p=2,3,4$, respectively. The *ab initio* calculations confirm the stability of such anions. Their structures optimized by the B3LYP DFT calculations are shown in Fig. 4. They have a strong resemblance to anion structures derived from the experimental data.[38] It is hardly reasonable to analyze the polarization properties of the isolated anions because of the strong counterion effect,[39] i.e., because of the strong dependence of the polarizability of the anions on the atomic structural environment in the lattice under study. However, it is worth noting that the calculated values of polarizability and third-order hyperpolarizability (see Table IV) show the same increase of the specific values along with increasing chain length. Hence, it can be suggested that the $\gamma_s(p)$ dependency for the $[Te_pO_{2p+1}]^{2-}$ chain anions can be approximated by the same Eq. (26) which was established for the Te_pO_{2p} chain molecules.

TABLE IV. Specific isotrope polarizability and hyperpolarizability of the $[Te_pO_{2p+1}]^{2-}$ anions.

Anion	α_s (a.u.)	γ_s (a.u.)
$[Te_2O_5]^{2-}$	40.0	2890
$[Te_3O_7]^{2-}$	41.0	20401
$[Te_4O_9]^{2-}$	41.5	26330

In Ref. 9, NLO susceptibilities $\chi^{(3)}$ were measured for $(100-x)TeO_2+xM_2O$ glass with $x=7.5,20,25$ for $M=$Li; $x=5,10,20$ for $M=$Na; and $x=7.5,15,20$ for $M=$K. A drastic decrease of $\chi^{(3)}$ at increasing modifier content was found for all these compounds. First of all, it should be emphasized that such a rapid decrease cannot be explained by the composition dependence hypothesis only. This hypothesis suggests that NLO susceptibilities of modifier oxides are negligible and the decrease of the $\chi^{(3)}$ values of composite compound is due to lowering of content of the TeO_2 constituent. According to this assumption, dependence of $\chi^{(3)}$ on x must be linear. This evidently contradicts experimental data of Ref. 9, which show that linear approximation of the $\chi^{(3)}\times(x)$ dependence would lead to a zero $\chi^{(3)}$ values at x equal to 33%, 37% and 50% for $M=$Li,Na,K, respectively. Note that the second factor which could affect the $\chi^{(3)}$ value, the volume dilatation induced by increase of modifier content, is of minor importance. According to experimental data of Ref. 9, such a dilatation is negative for $M=$Li, negligible for $M=$Na, and only amounts to 4% for $M=$K.

For each of these compounds, the number p can be evaluated from Eq. (30). In Fig. 5, the NLO susceptibilities $\chi^{(3)}$ measured in Ref. 9 are presented against p numbers jointly with theoretical $\gamma_s(p)$ specific hyperpolarizabilities fitted to those $\chi^{(3)}$ values by varying the parameters G and σ in Eq. (26).

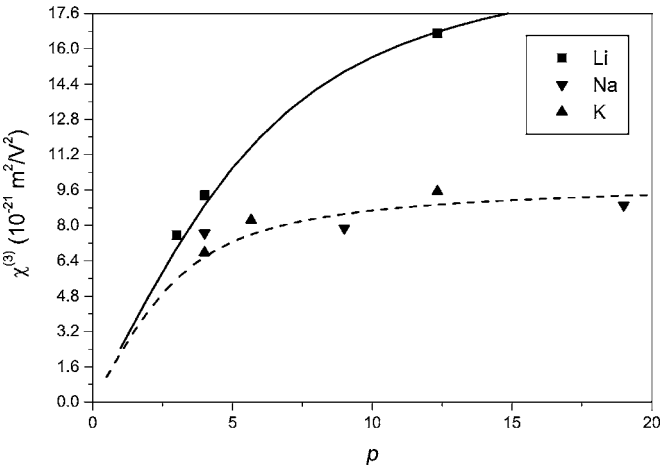

FIG. 5. NLO coefficients of tellurite glasses doped by Li_2O, Na_2O, and K_2O (experimental data from Ref. 9) as function of the chain length p calculated by Eq. (30). The lines show the $\gamma_s(p)$ dependencies calculated by Eq. (26) for $\sigma=10$ (solid line) and for 5 (dashed line).

Despite a limited number of available experimental data on the $\chi^{(3)}$ values of the alkali-metal-doped tellurite glass, they are sufficient to estimate the value of the σ parameters for each kind of glass. Therefore, it was found that the experimental composition dependencies of the $\chi^{(3)}$ values for the sodium and potassium tellurite glasses can be satisfactorily reproduced by the same $\gamma_s(p)$ function with $\sigma=5$ (dashed line), whereas the $\chi^{(3)}$ values for the Li_2O—TeO_2 glass obey the $\gamma_s(p)$ function with $\sigma=10$ (solid line).

In other words, the $p\rightarrow\infty$ limits of $\chi^{(3)}$ values for the glasses doped by Na_2O and K_2O (near 10×10^{-21} m^2/V^2 as it is seen in Fig. 5) are correctly simulated by the $\gamma_s(p)$ function, and coincide very closely with the value simulated by the $\gamma_s(p)$ found for pure TeO_2 glass [Fig. 3(c)], although the σ parameter of the former function is two times smaller than that of the latter. This calculation trick seems to be bizarre as well as the fact that the experimental $\chi^{(3)}$ values for the Li_2O-doped glass have a $p\rightarrow\infty$ limit two times higher than the one found for Na_2O- and K_2O-doped tellurite glass (see Fig. 5). Actually, such a limit has a well defined physical sense and therefore must have the same value for all modifiers. However, this does not hinder us from establishing that the above consideration can explain why the third-order susceptibility of the tellurite glass shows a nonlinear decrease with incresing quantity of modifier.

VI. CONCLUSIONS

The simulation of the extraordinary NLO susceptibility of TeO_2 glass using *ab initio* estimations of hyperpolarizabilties of various types of $(TeO_2)_p$ polymer molecule shows that only one type of such molecules, namely, chainlike species, seem to be capable of realistically reproducing the above mentioned properties due to the drastic augmentation of their specific (i.e., per one link) third-order hyperpolarizability with increasing chain length.

This property cannot be attributed to a local electronic response arising in the chain links under an applied electric field. On the contrary, this argues for an exceptionally strong nonlocality of the electronic polarization in these chains which can be considered as a particular physical factor inherent for them and dictating this property.

In general, the above mentioned points support the early hypothesis supposing that the chainlike $(TeO_2)_p$ polymers are similar to typical fragments of TeO_2 glass.

This naturally implies that the complex anions in the tellurite glass, originating from these fragments also have a chainlike constitution and its length remains the factor governing its hyperpolarizability. The model calculations based on this idea reproduce the experimental behaviors of the nonlinear susceptibilities in a series of tellurite glass with varying concentration of alkali-metal oxide modifier.

ACKNOWLEDGMENTS

This study was carried out while M.S. was an invited researcher in the SPCTS laboratory at Limoges University, and he would like to thank the staff for their hospitality and helpful discussions. This research was supported by the Centre National de la Recherche Scientifique (France).

*Author to whom correspondence should be addressed. Email address: andrei.mirgorodski@unilim.fr

[1] D. W. Hall, M. A. Newhause, N. F. Borelli, W. H. Dumaugh, and D. L. Weidman, Appl. Phys. Lett. **54**, 1293 (1988).
[2] H. Nasu, T. Uchigaki, K. Kmiya, and K. Kubodera, Jpn. J. Appl. Phys., Part 1 **3**, 3899 (1992).
[3] (a) S. H. Kim, T. Yoko, and S. Sakka, J. Am. Ceram. Soc. **76**, 865 (1993); (b) S. H. Kim and T. Yoko, *ibid.* **78**, 1061 (1995).
[4] H. Berthereau, Y. Le Luyer, R. Olazcuaga, G. Le Flem, M. Couzi, L. Canioni, P. Segonds, L. Sarger, and A. Ducasse, Mater. Res. Bull. **29**, 933 (1994).
[5] L. Canioni, M. O. Marti, B. Bousquet, and L. Sarger, Opt. Commun. **151**, 241 (1998).
[6] B. Jeansannetas, S. Blanchandin, P. Thomas, P. Marchet, J. C. Champarnaud-Mesjard, T. Merle-Mejean, B. Frit, V. Nazabal, E. Fargin, G. Le Flem, M. O. Marti, B. Bousquet, L. Canioni, S. Le Boiteux, P. Segonds, and L. Sarger, J. Solid State Chem. **146**, 329 (1999).
[7] S. Le Boiteux, P. Segonds, L. Canioni, L. Sarger, E. Fargin, T. Cardinal, C. Duchesne, and G. Le Flem, J. Appl. Phys. **81**, 14817 (1997).
[8] S.-H. Kim, T. Yoko, and S. Sakka, J. Am. Ceram. Soc. **76**, 2486 (1993).
[9] S.-H. Kim, J. Mater. Res. **14**, 1074 (1999).
[10] E. Fargin, H. Berthereau, T. Cardinal, G. Le Flem, L. Ducasse, L. Canioni, P. Segonds, L. Sarger, and A. Ducasse, J. Non-Cryst. Solids **203**, 96 (1996).
[11] J. Lin, W. Huang, Z. Sun, C. S. Ray, and D. E. Day, J. Non-Cryst. Solids **336**, 189 (2004).
[12] M. E. Lines, Phys. Rev. B **41**, 3372 (1990).
[13] M. E. Lines, Phys. Rev. B **41**, 3383 (1990).
[14] M. E. Lines, Phys. Rev. B **43**, 11978 (1991).
[15] S. Suehara, P. Thomas, A. P. Mirgorodsky, T. Merle-Mejean, J.-C. Champarnaud-Mesjard, T. Aizawa, S. Hishita, S. Todoroki, T. Konishi, and S. Inoue, Phys. Rev. B **70**, 205121 (2004).
[16] O. Noguera, M. Smirnov, A. P. Migorodsky, T. Merle-Mejean, P. Thomas, and J. C. Champarnaud-Mesjard, Phys. Rev. B **68**, 094203 (2003).
[17] O. Noguera, M. Smirnov, A. Mirgorodsky, T. Merle-Mejean, P. Thomas, and J. C. Champarnaud-Mesjard, J. Non-Cryst. Solids **345&346**, 734 (2004).
[18] V. G. Dmitriev, G. G. Guzardyan, G. G. Nikogosyan, and D. N. Germany, *Handbook of Non-Linear Optical Crystals* (Springer, Berlin, 1999).
[19] S. Suehara, P. Thomas, A. Mirgorodsky, T. Merle-Mesjean, J. C. Champarnaud-Mejard, T. Aizawa, S. Hishita, S. Todoroki, T. Konishi, and S. Inoue, J. Non-Cryst. Solids **345&346**, 730 (2004).
[20] R. Adair and L. L. Payne, J. Opt. Soc. Am. B **4**, 875 (1987).
[21] H. Sekino and R. J. Bartlett, J. Chem. Phys. **96**, 3022 (1993).

[22] A. D. Becke, J. Chem. Phys. **98**, 1372 (1993); C. Lee, W. Yang, and R. G. Parr, Phys. Rev. B **37**, 785 (1988).
[23] M. J. Frisch *et al.*, GAUSSIAN 98, Rev. A.9 (Gaussian, Inc., Pittsburgh, 1998).
[24] T. Uchino, S.-H. Kim, T. Yoko, and T. Fukunaga, J. Ceram. Soc. Jpn. **105**, 201 (1997).
[25] H. Nida, T. Uchino, J. Jin, S.-H. Kim, T. Fukunaga, and T. Yoko, J. Chem. Phys. **114**, 459 (2001).
[26] G. Pacchioni and C. Mazzeo, Phys. Rev. B **62**, 5452 (2000).
[27] T. Uchino, M. Takahashi, and T. Yoko, Appl. Phys. Lett. **79**, 359 (2001).
[28] O. V. Mazurin, M. V. Streltsina, and T. P. Shvaiko-Shvaikovskya, *Handbook of Glass Data* (Elsevier, New York, 1985).
[29] R. A. H. El-Mallawany, *Tellurite Glasses Handbook* (CRC Press, Boca Raton, FL, 2002).
[30] K. F. Zmbov, L. L. Ames, and J. L. Margrave, High. Temp. Sci. **5**, 235 (1973).
[31] D. W. Muenow, J. W. Hastie, R. Hauge, R. Bautista, and J. L. Margrave, Trans. Faraday Soc. **65**, 3210 (1969).
[32] T. Uchino, Y. Kitagawa, and T. Yoko, Phys. Rev. B **61**, 234 (2000).
[33] X. Yuan and A. N. Cormack, J. Non-Cryst. Solids **283**, 69 (2001).
[34] T. Uchino, Curr. Opin. Solid State Mater. Sci. **5**, 517 (2001).
[35] V. H. Beyer, Z. Kristallogr. **124**, 228 (1967).
[36] J. C. Champarnaud-Mesjard, S. Blanchandin, P. Thomas, A. Mirgorodsky, T. Merle-Mejean, and B. Frit, J. Phys. Chem. Solids **61**, 1499 (2000).
[37] O. Spirina-Jenkins and K. L. C. Hunt, J. Mol. Struct. **633**, 145 (2003).
[38] C. R. Becker, S. L. Tagg, J. C. Huffman, and J. W. Zwanziger, Inorg. Chem. **36**, 5559 (1997).
[39] T. R. Coundari, H. A. Kurtz, and T. Zhou, Chem. Phys. **240**, 205 (1999).